Volume 9, Issue 4, 2019, 4101 - 4106 ISSN 2069-5837

Biointerface Research in Applied Chemistry

www.BiointerfaceResearch.com

https://doi.org/10.33263/BRIAC94.101106

Original Research Article Open Access Journal

Received: 06.07.2019 / Revised: 09.08.2019 / Accepted: 10.08.2019 / Published on-line: 15.08.2019

Biomedical applications of bismuth oxide based nanocomposite: computed tomography and anticancer drug loading

Mohsen Zeini [1, 2], Baharak Divband [3, 4], Davood Khezerloo [2], Nahideh Gharehaghaji [2, *]

[1]Medical Radiation Sciences Research Group, Tabriz University of Medical Sciences, Tabriz, Iran
[2]Department of Radiology, Faculty of Paramedicine, Tabriz University of Medical Sciences, Tabriz, Iran
[3]Dental and Periodontal Research Center, Tabriz University of Medical Sciences, Tabriz, Iran
[4]Inorganic Chemistry Department, Chemistry Faculty, University of Tabriz, C.P. 51664 Tabriz, Iran

*corresponding author e-mail address: ***gharehaghajin@tbzmed.ac.ir***

ABSTRACT

Today, computed tomography (CT) has a special place among medical imaging modalities. Conventional intravascular contrast agents of CT have a short blood half-life and make adverse reactions. To overcome the problems, recently, nanomaterials with high capabilities for diagnostic and therapeutic purposes have been developed as CT contrast agents. In this study, bismuth oxide/bovine serum albumin/5-Fluorouracil nanocomposite was synthesized and characterized to investigate its efficiency for contrast enhancement of CT imaging as well as loading anticancer drug. CT was performed using 256 slices dual source clinical scanner with both single and dual source mode. The effect of bismuth oxide/bovine serum albumin nanocomposite and its 5-Fluorouracil loaded form on cell viability of A549 cell line was investigated. The average size of the nanocomposite was measured around 20-30 nm. The X-ray attenuation ability of the nanocomposite in single and dual CT imaging was obtained more than 2000 Hounsfield units (HU) in the highest concentration. In similar concentrations, the CT contrast enhancement of the nanocomposite was 1.2 times higher than Iohexol (Omnipaque) as conventional CT contrast agent. 5-Fluorouracil loaded nanocomposite showed 63% killing of cancer cells while the unloaded nanocomposite showed high cytocompatibility even at the highest concentration. This study offers the novel bioapplication of synthetic bismuth oxide/bovine serum albumin/5-Fluorouracil nanocomposite as a potential contrast agent in CT with capability for anticancer drug loading.

Keywords: *Computed Tomography, Nanocomposite, X-Ray Attenuation, Contrast, Anticancer Drug Loading.*

1. INTRODUCTION

X-ray computed tomography (CT) is one of the most usable and available tools in medical imaging [1].CT provides three-dimensional images instead of two-dimensional radiography and overcomes the problem of overlapping anatomical structures in conventional radiography. Comparing with MRI and PET, CT has a higher temporal and spatial resolution but lower sensitivity. Moreover, CT is more abundantly available and has a lower cost than those modalities [2]. Dual energy computed tomography (DECT) is a technique that combines imaging information acquired with two different X-ray energies. Subsequently, Photoelectric and Compton effects analyzed; and therefore, it enables to material differentiation [3]. There are different acquisition methods to produce dual energy. One of these methods is using of dual source computed tomography (DSCT) [4]. Dual source scanners have two separate tubes for high and low kVp with a ~90° angle to each other. High kVp tube has a fixed kVp (140 or 150) depending on scanner model. On the other hand, low kVp tube depends on the examination type and patient size can operate at different kVps from 70 to 100 kVp [5]. The third generation of DSCT has added some new features such as produce of higher X-ray tube currents, a thicker tin filter for the high kVp tube and additional dual energy tube voltage [6].

Image contrast of CT depends on attenuation of X-ray beam during photons pass through patient's body and intensity of X-ray beam reduces. X-ray attenuation is related to the attenuation coefficient (μ) as following equation:

$$\mu = \frac{\rho Z^4}{AE^3} \qquad \text{Equation 1}$$

Where ρ is density, Z is atomic number and A is atomic mass of the material. E is related to the X-ray energy [7].CT contrast media employ materials with high atomic number. Iodine (I) based contrast agents and oral barium sulfate ($BaSO_4$) are the commonly used contrast materials for CT. However, usage of iodized contrast agents in many cases can lead to allergic reactions [8]. Additionally, iodine based agents have a short blood half-life which limits the time of imaging [9]. To overcome the problems, high atomic number nanomaterials such as bismuth (Bi), gold (Au), gadolinium (Gd) and others have been investigated for CT in recent years [10]. These nanomaterials can passively accumulate at the tumor site, prolong circulation time for in vivo experiments, provide easy surface modification [11] and allow to spectral CT imaging [12]. Bismuth based nanoparticles have attracted great attention for CT imaging. Bismuth nanoparticles and bismuth oxide (Bi_2O_3) [13], bismuth sulfide (Bi_2S_3) [14] and bismuth selenide (Bi_2Se_3) [15]forms have been investigated as a part of nanostructures which used for CT contrast enhancement. Comparing to iodine (Z=53), bismuth nanoparticles (Z=83) have advantages of higher atomic number, lower toxicity and cost [16]. Besides, bismuth has higher attenuation coefficient (5.74 cm^2kg^{-1} at 100 KeV) than iodine (1.94 cm^2kg^{-1} at 100 KeV) [17] and shows fewer changes in CT value across various kVp settings relative to iodine and barium [18]. In addition to intravenous administration

of bismuth based nanostructures, they have been used as oral contrast agent for imaging of the gastrointestinal tract [19].

Bovine serum albumin (BSA) is a protein which is usually used as a template for preparation of nanocomposites. Because of high number of binding sites, BSA has a high potential to bind many drug moieties comparing to other substrates [20]. In addition, BSA has excellent biocompatibility, and good water solubility and colloidal stability[21].BSA commonly uses for the surface modification of nanoparticles [22]. Therefore, BSA has a large application in various types of imaging modalities, especially CT scan. For instance, in a study, BSA@Bi_2S_3 nanoparticles were compared with $BaSO_4$ in vitro and showed higher CT value. Besides, orally administered BSA@Bi_2S_3 nanoparticles were introduced as a promising agent for 3D CT imaging of gastrointestinal tract of mice [23]. In other study, BSA-Au nanoclusters were used for 2D and 3D CT imaging for visualization of mouse kidney and diagnosing of disease [24].

5-Fluorouracil (5FU) is an anticancer drug which inhibits DNA formation with blockage of the thymidylatesynthetase enzyme [25]. It is used to treatment of ocular [25], head and neck, colorectal and breast cancers [26]. Comparing to other anticancer agents such as IFN (interferon alfa-2b) and MMC (mitomycin C), 5FU has lower frequent dosing regimen and cancer treatment cost. Moreover, its solutions are stable at 25°C for several weeks [25].

So far, different bismuth based nanoparticles have been investigated for CT imaging.Hyaluronic acid-functionalized Bi_2O_3 (HA-Bi_2O_3) nanoparticles have been introduced as a theranostic agent for CT guided radiotherapy [13]. Polyvinylpyrrolidone (PVP) coated porous bismuth (pBi) nanospheres with doxorubicin (DOX) have shown theranostic properties for CT and combined photothermal therapy, radiotherapy and chemotherapy [27]. Besides, polydopamine (PDA)/HSA/DOX coated bismuth selenide (Bi_2Se_3) nanoparticles have been also introduced as multifunctional agent for CT and infrared thermal imaging as well as thermo-chemotherapy [15]. However, based on our knowledge, integration of Bi_2O_3 nanoparticles, BSA and 5FU in the form of Bi_2O_3/BSA/5FU nanocomposite has not been investigated as a CT contrast agent with capability for loading of 5FU.

The aim of this study was the synthesis of novel Bi_2O_3/BSA/5FU nanocomposite and investigation of its potential for CT imaging and 5FU anticancer agent loading applications.

2. MATERIALS AND METHODS

2.1. Chemistry.

Bismuth (III) nitrate ($Bi(NO_3)_3$), nitric acid (HNO_3), citric acid ($C_6H_8O_7$), bovine serum albumin (BSA), 5-Fluorouracil, poly ethylene glycol (PEG) 4000, ammonia (NH_3) and ethanol (96%) were supplied by Merck.

2.2. Synthesis of Bi_2O_3/BSA/5FU nanocomposite.

In the first step, Bi_2O_3 nanoparticles were synthesized using a polymer degradation technique in which 4.6 g $Bi(NO_3)_3$ was dissolved in nitric acid (2M), then 20 ml of acid citric (1M) was added to the solution and stirred for 2 hours. Next, distilled water was added to the solution to reach 135 ml in volume. Then PEG was added to the solution and stirred for 2 hours. Finally, with the help of ammonia (NH_3), the pH of the whole solution was fixed at 9. Gradually, yellow color sediment was obtained by increasing the pH, and then by adding distilled water and ethanol the impurities were washed. The resulting product was dried at 80 °C and calcinated for 3 hours at 500 °C, the obtained nanoparticles were bismuth oxide (Bi_2O_3).

For the synthesis of Bi_2O_3/BSA nanoparticles in a typical process, BSA was selected as a template protein. In this level, the certain amount of BSA and ascorbic acid were added to Bi_2O_3 nanoparticles and the bonding of these materials was completed by ultrasound and 45° C. The final product was separated and washed by centrifuge, and Bi_2O_3/BSA nanoparticles were produced.

5FU-loaded Bi_2O_3/BSA nanoparticles were prepared as described elsewhere [28]. Briefly, 0.2 g Bi_2O_3/BSA in 2.0 mL aqueous drug solution, titrated to the desired pH and incubated at room temperature. It was converted to the nanoparticles by adding ethanol as a desolvating agent, at the rate of 1.0 mL/min and under stirring (550 rpm) at room temperature. Then,the cross-linking process was performed by addingglutaraldehyde aqueous solution (8% w/w) to induce particle cross-linking under stirring overnight. The final product was Bi_2O_3/BSA/5FU nanocomposite.

2.3. Measurements.

X-Ray diffractometry (XRD: Philips diffractometer), transmission electron microscopy (TEM: Zeiss LEO 912 Omega) and MAP of scanning electron microscopy (Philips ES 30 KW) were done for Bi_2O_3/BSA/5FU to determine the physicochemical properties of the nanocomposite.

2.4. MTT (methyl thiazolyltetrazolium) assay.

In this study, in vitro cytotoxicity of the nanocomposite was checked out by using the typical methyl thiazolyltetrazolium (MTT) assay on A549 alveolar adenocarcinoma cells. The cells were incubated in 96-well plates (8×10^3 cells per well) and cultured at 5% CO_2 and 37° C for 24 hours. Different concentrations of the nanocomposite (0.06, 0.11, 0.14, 0.18, 0.22 mM) were added to the culture media and the cells incubated for 24 hours. Then, 50 µL of 2 mg/ml MTT solution and 150 µL culture medium were added to each well and incubation was carried out for a 4 hours at 37° C and 5% CO_2. In the next step, plate wells were washed withPhosphate-buffered solution and residual media removed. After adding dimethyl sulfoxide and Sorensonbuffer as solubilizer to each well, the absorbance was measured at 570 nm using an ELISA plate reader (BioTeck, Bad Friedrichshall, Germany).

2.5. CT protocol and imaging.

Different concentrations (6, 12, 24, 36 and 50 mg/ml) of Bi_2O_3/BSA/5FU and Iohexol (Omnipaque, New York, USA) as conventional CT contrast agent were prepared. CT was performed at 18° C using 256 slices (2×128) dual source clinical scanner (SOMATOM Definition Flash – CT scanner – Siemens Healthiness Global, Germany) to prepare single and dual source imaging. The parameters of the single source imaging were as

follow: kVp: 120, mAs: 110, scan time: 1.13 s, rotation time: 0.28 s, FOV: 250 mm^2, Pitch: 0.5, increment: 0.6, slice thickness (collimation): 128×0.6 mm. The Hounsfield units of the samples were obtained for all concentrations of the nanocomposite and Iohexol using CT scanner workspace. The above steps were repeated with dual source scanner using 80 and 140 kVp and 0.28 s rotation time.

3. RESULTS

3.1. Measurements.

XRD pattern showed the peaks related to Bi_2O_3/BSA/5FU (figure 1) confirming the succes synthesis of the nanocomposite.

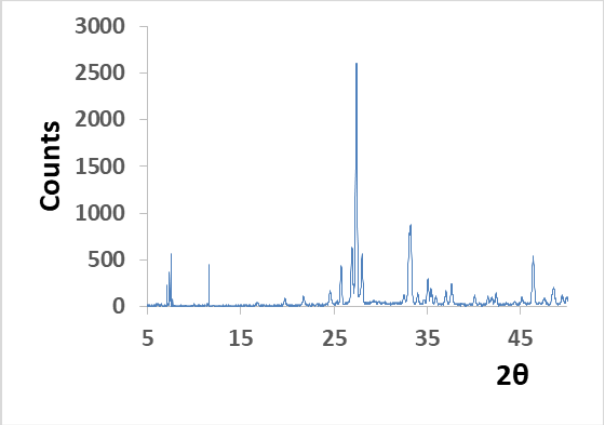

Figure 1. XRD pattern of Bi_2O_3/BSA/5FU nanocomposite.

TEM image indicated the average size of the nanocomposite was 20-30 nm (figure 2). The size was higher than the threshold for filtration of kidneys, therefore, the blood half-life of the nanocomposite is enough high to provide appropriate imaging time.

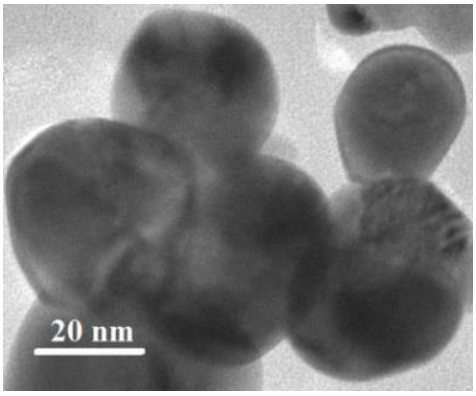

Figure 2. TEM image of Bi_2O_3/BSA/5FU nanocomposite.

The homogenous dispersion of Bi, carbon (C) and oxygen (O) in the Bi_2O_3/BSA/5FU was shown by MAP in figure 3. The figure illustrates higher amounts of carbon (figure 3B) compared to oxygen (figure 3C) and bismuth (figure 3A) in the nanocomposite. This finding is related to the presence of carbon in the structure of BSA and 5FU. Although oxygen exists in the structure of Bi_2O_3, BSA and 5FU, its amount is lower than carbon. On the other hand, Bi amount in the nanocomposite was less than other elements. This finding is in agreement with the TEM results. Bismuth atoms are seen as dark points in the TEM image (figure 2) because of its high atomic number while carbon and oxygen form bright points. Therefore, the dark area of the figure is less than the bright area.

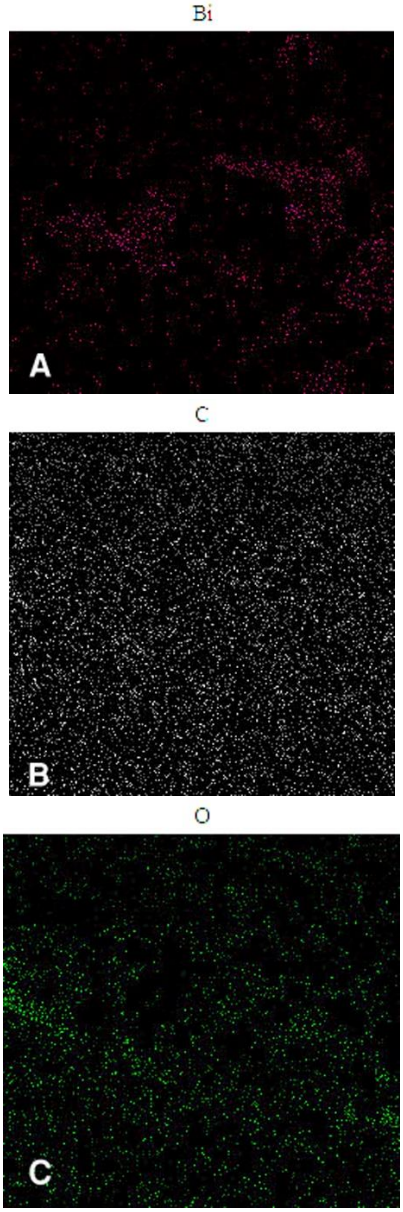

Figure 3. MAP of A) Bismuth, B) Carbon and C) Oxygen.

3.2. MTT assay.

Figure 4 demonstrated the MTT assay results for Bi_2O_3/BSA/5FU and Bi_2O_3/BSA. Decreasing of cell viability as a function of both nanocomposites concentration is seen in the figure. The cell viability of Bi_2O_3/BSA/5FU was lower than Bi_2O_3/BSA nanocomposite for all of the concentrations. At the first part of the chart (low concentrations up to 0.14 mM), the differences between the two nanostructures were low but it was significant for higher concentrations. This phenomena is related to the low amount of 5FU loading and subsequently lower release of the drug. For Bi_2O_3/BSA nanocomposite, the cell viability for all concentrations was higher than 80%, confirming its high compatibility for cell

culture. On the other hand, the cell viability with Bi_2O_3/BSA/5FU nanocomposite was higher than 80% only for the lowest concentration (0.11 mM). The cell killing effect was increased with increasing Bi_2O_3/BSA/5FU nanocomposite concentration, so that, it was 63% for concentration of 0.22 mM. This finding confirms the successful loading of 5FU to Bi_2O_3/BSA nanocomposite that leads to high capacity of the Bi_2O_3/BSA/5FU for killing A549 alveolar adenocarcinoma cancer cells.

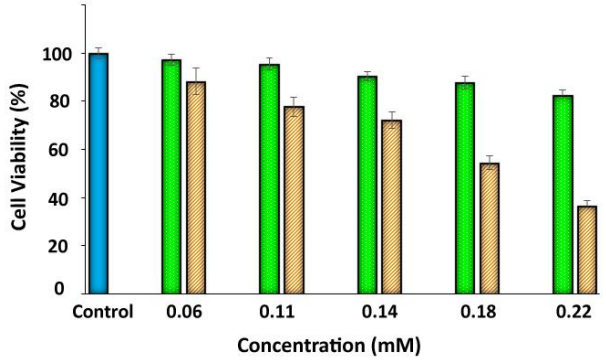

Figure 4. A549 alveolar adenocarcinoma cell viability after incubation with different concentrations of Bi_2O_3/BSA/5FU (dashed columns) and Bi_2O_3/BSA (green solid columns)nanocomposites.

3.3. Phantom imaging.

Figure 5 illustrates the phantom images of Bi_2O_3/BSA/5FU nanocomposite (5A) and Iohexol (5B) at different concentrations prepared with single source CT. According to the figure, as the concentration of the nanocomposite and Iohexol was step by step increased, the X-ray attenuation of the samples, and therefore, the brightness of the images were also increased. However, in similar concentrations, the brightness for Bi_2O_3/BSA/5FU was higher than that of Iohexol as conventional CT contrast agent. Figure 5C shows the plot of CT value (HU) versus concentration for the samples. The amount of X-ray attenuation for the both substances was increased linearly with increasing of concentration, but higher line slope was obtained using Bi_2O_3/BSA/5FU nanocomposite.

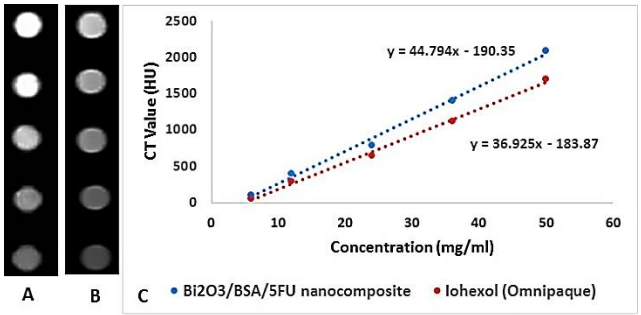

Figure 5. Phantom images of A) Bi_2O_3/BSA/5FU nanocomposite, and B) Iohexol, C) The plot of CT value versus concentration forBi_2O_3/BSA/5FU nanocomposite and Iohexol.

Increasing of the nanocomposite concentration leads to increasing Bi_2O_3 content in the samples. Therefore, change in the mass ratio between Bi_2O_3 and water molecules makes concentration-dependent effect. Iohexol is an iodine based contrast agent which is widely used for contrast enhanced CT. Since bismuth has higher atomic number than iodine (Z=83 for bismuth and 53 for iodine), based on equation one, attenuation coefficient (μ) for Bi_2O_3/BSA/5FU nanocomposite is higher than the iodine based contrast agent. Therefore, bismuth oxide based nanocomposite indicates higher X-ray attenuation. The linearity between CT values and concentrations of the nanocomposite with high slope reveals high efficiency of the nanocomposite for enhancing of CT contrast. Thus, the nanocomposite can provide equal X-ray attenuation in lower doses comparing to the conventional iodine based contrast agent. Moreover, our nanocomposite benefits from loading of 5FU as anticancer drug. Comparing to other Bi_2O_3 based nanostructure, X-ray attenuation of Bi_2O_3/BSA/5FU nanocomposite is higher than hyaluronic acid-functionalized bismuth oxide (HA-Bi_2O_3) nanoparticles [13] in similar concentrations.

The graph of X-ray attenuation at different concentrations of Bi_2O_3/BSA/5FU nanocomposite produced by 80 and 140 kVp voltages in dual source CT is shown in figure 6. Increasing of X-ray attenuation as a function of concentration is seen for the both kilovoltages. Although high X-ray attenuation was obtained for both of the voltages, the CT values for 80 kVp was higher than 140 kVp in similar concentrations.

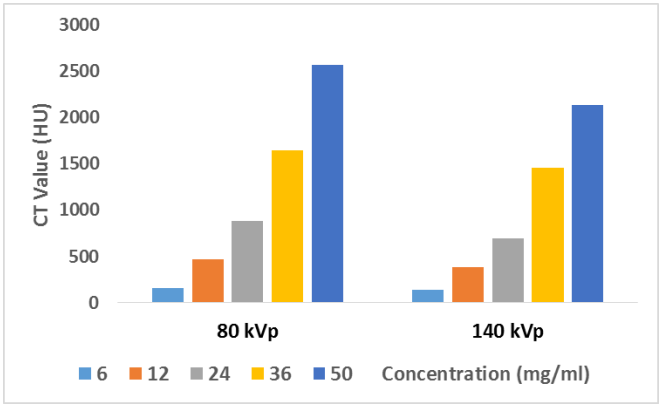

Figure 6. X-ray attenuation at different concentrations of Bi_2O_3/BSA/5FU nanocomposite produced by 80 and 140 kVp in dual source CT.

Based on equation 1, the attenuation coefficient is proportional to the third power of energy. Therefore, decreasing in attenuation coefficient occurs when energy increases from 80 to 140 kVp. Although differences of CT values are seen between 80 and 140 kVp, confirming the capability of Bi_2O_3/BSA/5FU nanocomposite for DSCT needs more investigations. Comparison the results of DSCT in the present study with a study [29]on Bi using 80 and 140 kVp shows slightly higher X-ray attenuation for Bi_2O_3/BSA/5FU nanocomposite.

The results of this study indicate that Bi_2O_3/BSA/5FU nanocomposite has a high potential to use as CT contrast agent with capability of loading 5FU as anticancer drug. Additionally, the results can be used to design future in vivo study in animal model. Since the nanocomposite size is higher than 8nm (threshold for glomerular filtration), the nanocomposite is not rapidly excreted by the kidneys [30], and therefore, it may be useful to detect liver lesions in future in vivo studies. Additionally, the nanocomposite size and hydrophilic property provide its longer stay in blood circulatory system and there will be a longer imaging time for X-ray imaging modalities.

4. CONCLUSIONS

As a conclusion, in this in vitro study, Bi_2O_3/BSA/5-Fluorouracil nanocomposite was successfully synthesized and characterized to consider its efficiency to attenuate X-rays with the photon energies used in single and dual source CT scan as well as loading anticancer drug. According to the high X-ray attenuation of the nanocomposite compared to the conventional iodinated contrast agent, it has a good potential to use for contrast enhanced CT imaging. The nanocomposite also showed high capability of killing alveolar adenocarcinoma cancer cells. Usage of Bi_2O_3/BSA/5-Fluorouracil for CT imaging in animal model and investigation of the nanocomposite capability as a drug delivery system can be done as future research works.

5. REFERENCES

1. Veintemillas-Verdaguer, S.; Luengo, Y.; Serna, C.J.; Andres-Verges, M.; Varela, M.; Calero, M.; Lazaro-Carrillo, A.; Villanueva, A.; Sisniega, A.; Montesinos, P.; Morales, M. P. Bismuth labeling for the CT assessment of local administration of magnetic nanoparticles. *Nanotechnology* **2015,** *26*, 135101.
2. Cole, L. E.; Ross, R. D.; Tilley, J. M.; Vargo-Gogola, T.; Roeder, R. K. Gold nanoparticles as contrast agents in x-ray imaging and computed tomography. *Nanomedicine (Lond)* **2015,** *10*, 321-41, https://doi.org/10.2217/nnm.14.171.
3. Fornaro, J.; Leschka, S.; Hibbeln, D.; Butler, A.; Anderson, N.; Pache, G.; Scheffel, H.; Wildermuth, S.; Alkadhi, H.; Stolzmann, P., Dual- and multi-energy CT: approach to functional imaging. *Insights Imaging* **2011,** *2*, 149-159, https://doi.org/10.1007/s13244-010-0057-0.
4. Goo, H.W.; Goo, J.M. Dual-Energy CT: New Horizon in Medical Imaging. *Korean J Radiol* **2017,** *18*, 555-569, https://doi.org/10.3348/kjr.2017.18.4.555.
5. Megibow, A.J.; Kambadakone, A.; Ananthakrishnan, L. Dual-Energy Computed Tomography: Image Acquisition, Processing, and Workflow. *Radiol Clin North Am* **2018,** *56*, 507-520.
6. Wichmann, J.L.; Hardie, A.D.; Schoepf, U.J.; Felmly, L.M.; Perry, J.D.; Varga-Szemes, A.; Mangold, S.; Caruso, D.; Canstein, C.; Vogl, T.J.; De Cecco, C.N. Single- and dual-energy CT of the abdomen: comparison of radiation dose and image quality of 2nd and 3rd generation dual-source CT. *Eur Radiol* **2017,** *27*, 642-650, https://doi.org/10.1007/s00330-016-4383-6.
7. Hernandez-Rivera, M.; Kumar, I.; Cho, S.Y.; Cheong, B.Y.; Pulikkathara, M.X.; Moghaddam, S.E.; Whitmire, K.H.; Wilson, L.J. High-Performance Hybrid Bismuth-Carbon Nanotube Based Contrast Agent for X-ray CT Imaging. *ACS Appl Mater Interfaces* **2017,** *9*, 5709-5716, https://doi.org/10.1021/acsami.6b12768.
8. Dewachter, P.; Laroche, D.; Mouton-Faivre, C.; Bloch-Morot, E.; Cercueil, J.P.; Metge, L.; Carette, M. F.; Vergnaud, M. C.; Clement, O., Immediate reactions following iodinated contrast media injection: a study of 38 cases. *Eur J Radiol* **2011,** *77*, 495-501, https://doi.org/10.1016/j.ejrad.2009.09.019.
9. Hallouard, F.; Anton, N.; Choquet, P.; Constantinesco, A.; Vandamme, T. Iodinated blood pool contrast media for preclinical X-ray imaging applications--a review. *Biomaterials* **2010,** *31*, 6249-68, https://doi.org/10.1016/j.biomaterials.2010.04.066.
10. Cormode, D.P.; Naha, P.C.; Fayad, Z.A. Nanoparticle contrast agents for computed tomography: a focus on micelles. *Contrast Media Mol Imaging* **2014,** *9*, 37-52, https://doi.org/10.1002/cmmi.1551.
11. Liu, Y.; Ai, K.; Lu, L. Nanoparticulate X-ray computed tomography contrast agents: from design validation to in vivo applications. *Acc Chem Res* **2012,** *45*, 1817-27, https://doi.org/10.1021/ar300150c.
12. Cormode, D.P.; Roessl, E.; Thran, A.; Skajaa, T.; Gordon, R.E.; Schlomka, J.P.; Fuster, V.; Fisher, E.A.; Mulder, W.J.; Proksa, R.; Fayad, Z.A. Atherosclerotic plaque composition: analysis with multicolor CT and targeted gold nanoparticles. *Radiology* **2010,** *256*, 774-82, https://doi.org/10.1148/radiol.10092473.
13. Du, F.; Lou, J.; Jiang, R.; Fang, Z.; Zhao, X.; Niu, Y.; Zou, S.; Zhang, M.; Gong, A.; Wu, C. Hyaluronic acid-functionalized bismuth oxide nanoparticles for computed tomography imaging-guided radiotherapy of tumor. *Int J Nanomedicine* **2017,** *12*, 5973-5992, https://doi.org/10.2147/IJN.S130455.
14. Huang, H.H.; Chen, J.; Meng, Y.Z.; Yang, X.Q.; Zhang, M.Z.; Yu, Y.; Ma, Z.Y.; Zhao, Y.D. Synthesis and characterization of Bi2S3 composite nanoparticles with high X-ray absorption. *Materials Research Bulletin* **2013,** *48*, 3800-3804, https://doi.org/10.1016/j.materresbull.2013.05.091.
15. Li, Z.; Hu, Y.; Howard, K.A.; Jiang, T.; Fan, X.; Miao, Z.; Sun, Y.; Besenbacher, F.; Yu, M. Multifunctional Bismuth Selenide Nanocomposites for Antitumor Thermo-Chemotherapy and Imaging. *ACS Nano* **2016,** *10*, 984-97, https://doi.org/10.1021/acsnano.5b06259.
16. Rabin, O.; Perez, J.; Grimm, J.; Wojtkiewicz, G.; Weissleder, R. An X-ray computed tomography imaging agent based on long-circulating bismuth sulphide nanoparticles. *Nat Mater* **2006,** *5*, 118-22, https://doi.org/10.1038/nmat1571.
17. Ai, K.; Liu, Y.; Liu, J.; Yuan, Q.; He, Y.; Lu, L. Large-scale synthesis of Bi(2)S(3) nanodots as a contrast agent for in vivo X-ray computed tomography imaging. *Adv Mater* **2011,** *23*, 4886-91, https://doi.org/10.1002/adma.201103289.
18. Yeh, B.M.; Fitz G.P.F.; Edic, P.M.; Lambert, J.W.; Colborn, R.E.; Marino, M.E.; Evans, P.M.; Roberts, J.C.; Wang, Z.J.; Wong, M.J.; Bonitatibus, P.J., Jr. Opportunities for new CT contrast agents to maximize the diagnostic potential of emerging spectral CT technologies. *Adv Drug Deliv Rev* **2017,** *113*, 201-222, https://doi.org/10.1016/j.addr.2016.09.001.
19. Zheng, X.; Shi, J.; Bu, Y.; Tian, G.; Zhang, X.; Yin, W.; Gao, B.; Yang, Z.; Hu, Z.; Liu, X.; Yan, L.; Gu, Z.; Zhao, Y. Silica-coated bismuth sulfide nanorods as multimodal contrast agents for a non-invasive visualization of the gastrointestinal tract. *Nanoscale* **2015,** *7*, 12581-91, https://doi.org/10.1039/c5nr03068d.
20. Huang, H.; Yang, D.P.; Liu, M.; Wang, X.; Zhang, Z.; Zhou, G.; Liu, W.; Cao, Y.; Zhang, W.J.; Wang, X. pH-sensitive Au-BSA-DOX-FA nanocomposites for combined CT imaging and targeted drug delivery. *Int J Nanomedicine* **2017,** *12*, 2829-2843, https://doi.org/10.2147/IJN.S128270.
21. Zhao, W.; Wang, Z.; Chen, L.; Huang, C.; Huang, Y.; Jia, N. A biomimetic Au@BSA-DTA nanocomposites-based contrast agent for computed tomography imaging. *Mater Sci Eng C Mater Biol Appl* **2017,** *78*, 565-570, https://doi.org/10.1016/j.msec.2017.04.127.
22. Guo, Z.; Zhu, S.; Yong, Y.; Zhang, X.; Dong, X.; Du, J.; Xie, J.; Wang, Q.; Gu, Z.; Zhao, Y. Synthesis of BSA-Coated

$BiOI@Bi_2S_3$ Semiconductor Heterojunction Nanoparticles and Their Applications for Radio/Photodynamic/Photothermal Synergistic Therapy of Tumor. *Adv Mater* **2017,** *29*, https://doi.org/10.1002/adma.201704136.
23. Zu, Y.; Yong, Y.; Zhang, X.; Yu, J.; Dong, X.; Yin, W.; Yan, L.; Zhao, F.; Gu, Z.; Zhao, Y. Protein-directed synthesis of Bi_2S_3 nanoparticles as an efficient contrast agent for visualizing the gastrointestinal tract. *RSC Advances* **2017,** *7*, 17505-17513, http://dx.doi.org/10.1039/C7RA01526G.
24. Wang, Y.; Xu, C.; Zhai, J.; Gao, F.; Liu, R.; Gao, L.; Zhao, Y.; Chai, Z.; Gao, X. Label-free Au cluster used for in vivo 2D and 3D computed tomography of murine kidneys. *Anal Chem* **2015,** *87*, 343-5, https://doi.org/10.1021/ac503887c.
25. Joag, M.G.; Sise, A.; Murillo, J.C.; Sayed-Ahmed, I.O.; Wong, J.R.; Mercado, C.; Galor, A.; Karp, C.L. Topical 5-Fluorouracil 1% as Primary Treatment for Ocular Surface Squamous Neoplasia. *Ophthalmology* **2016,** *123*, 1442-8, https://doi.org/10.1016/j.ophtha.2016.02.034.
26. Zoli, W.; Ulivi, P.; Tesei, A.; Fabbri, F.; Rosetti, M.; Maltoni, R.; Giunchi, D.C.; Ricotti, L.; Brigliadori, G.; Vannini, I.; Amadori, D. Addition of 5-fluorouracil to doxorubicin-paclitaxel sequence increases caspase-dependent apoptosis in breast cancer cell lines. *Breast Cancer Res* **2005,** *7*, 681-9, https://doi.org/10.1186/bcr1274.
27. Ma, G.; Liu, X.; Deng, G.; Yuan, H.; Wang, Q.; Lu, J. A novel theranostic agent based on porous bismuth nanosphere for CT imaging-guided combined chemo-photothermal therapy and radiotherapy. *Journal of Materials Chemistry B* **2018,** *6*, 6788-6795, http://dx.doi.org/10.1039/C8TB02189A.
28. Yu, S.; Gao, X.; Baigude, H.; Hai, X.; Zhang, R.; Gao, X.; Shen, B.; Li, Z.; Tan, Z.; Su, H., Inorganic nanovehicle for potential targeted drug delivery to tumor cells, tumor optical imaging. *ACS Appl Mater Interfaces* **2015,** *7*, 5089-96, https://doi.org/10.1021/am507345j.
29. Falt, T.; Soderberg, M.; Wasselius, J.; Leander, P. Material Decomposition in Dual-Energy Computed Tomography Separates High-Z Elements From Iodine, Identifying Potential Contrast Media Tailored for Dual Contrast Medium Examinations. *J Comput Assist Tomogr* **2015,** *39*, 975-80, https://doi.org/10.1097/RCT.0000000000000298.
30. Longmire, M.; Choyke, P.L.; Kobayashi, H. Clearance properties of nano-sized particles and molecules as imaging agents: considerations and caveats. *Nanomedicine (Lond)* **2008,** *3*, 703-17, https://doi.org/10.2217/17435889.3.5.703.

6. ACKNOWLEDGEMENTS

This work was adapted from MSc thesis and supported by Medical Radiation Sciences Research Group (MRSRG), Tabriz University of Medical Sciences (Grant No: 1397.121).The authors would like to thank Mr. Bahram Faraji for the assistance in preparation high resolution figures.